THE JOURNAL OF BIOLOGICAL CHEMISTRY VOL. 281, NO. 43, pp. 32728–32740, October 27, 2006

Fragment-based Screening of the Donor Substrate Specificity of Human Blood Group B Galactosyltransferase Using Saturation Transfer Difference NMR*[S]

Received for publication, January 17, 2006, and in revised form, July 11, 2006 Published, JBC Papers in Press, August 21, 2006, DOI 10.1074/jbc.M600424200

Astrid Blume[‡], Jesus Angulo[‡1], Thorsten Biet[‡], Hannelore Peters[‡], Andrew J. Benie[‡], Monica Palcic[§], and Thomas Peters[‡2]

From the [‡]Institute of Chemistry, University of Luebeck, Ratzeburger Allee 160, 23538 Luebeck, Germany and the [§]Carlsberg Laboratory, Gamle Carlsberg Vej 10, DK-2500 Valby, Denmark

Saturation transfer difference NMR experiments on human blood group B α-(1,3)-galactosyltransferase (GTB) for the first time provide a comprehensive set of binding epitopes of donor substrate analogs in relation to the natural donor UDP-Gal. This study revealed that the enzyme binds several UDP-activated sugars, including UDP-Glc, UDP-GlcNAc, and UDP-GalNAc. In all cases, UDP is the dominant binding epitope. To identify the minimum requirements for specific binding, a detailed analysis utilizing a fragment-based approach was employed. The binding of donor substrate to GTB is essentially controlled by the base as a "molecular anchor." Uracil represents the smallest fragment that is recognized, whereas CDP, AMP, and GDP do not exhibit any significant binding affinity for the enzyme. The ribose and β-phosphate moieties increase the affinity of the ligands, whereas the pyranose sugar apparently weakens the binding, although this part of the molecule controls the specificity of the enzyme. Accordingly, UDP represents the best binder. The binding affinities of UDP-Gal, UDP-Glc, and UMP are about the same, but lower than that of UDP. Furthermore, we observed that β-D-galactose and α-D-galactose bind weakly to GTB. Whereas β-D-galactose binds to the acceptor and donor sites, it is suggested that α-D-galactose occupies a third hitherto unknown binding pocket. Finally, our experiments revealed that modulation of enzymatic activity by metal ions critically depends on the total enzyme concentration, raising the question as to which of the bivalent metal cations Mg^{2+} and Mn^{2+} is more relevant under physiological conditions.

Complex carbohydrates play a key role in many biological processes such as cell migration, cell signaling, and cell-cell recognition. For the biological function of a glycoprotein or a glycolipid, the terminal glycosylation patterns are especially important because they are vital to potential molecular recognition reactions. Consequently, there is an enhanced interest in glycosyltransferases that are responsible for the biosynthesis of terminal glycan chains. The human blood group B galactosyltransferase is one of these "terminal" glycosyltransferases. Glycosyltransferases catalyze a regio- and stereospecific transfer of a single monosaccharide unit from a nucleotide donor to a hydroxyl group of an acceptor such as a saccharide, lipid, protein, or natural product. Glycosyltransferases are highly specific for their donor and acceptor substrates and have been grouped into over 80 families according to their amino acid sequences (1, 2). With few exceptions, a single glycosyltransferase is required for each individual glycosidic linkage. It is estimated that over 100 different glycosyltransferases are required to synthesize all of the reported oligosaccharides on glycoproteins and glycolipids (3). Although no extensive sequence similarities have been identified among different families of glycosyltransferases, human blood group A and B galactosyltransferases have almost identical amino acid sequences, differing only in four amino acids of 354 (4, 5), yet the two enzymes have clearly distinct donor substrate specificities.

The histo-blood group ABO(H) antigens are carbohydrate determinants found mainly on the surface of red blood cells and are largely responsible for mismatched blood transfusions. ABO carbohydrate antigens also occur on the surface of other cell types and are important in cell development, cell differentiation, and oncogenesis (6–8). Blood group A individuals express α-(1,3)-*N*-acetylgalactosaminyltransferase (GTA[3]; EC 2.4.1.40), which catalyzes the transfer of GalNAc from the donor substrate UDP-GalNAc to the acceptor α-L-Fuc-(1,2)-β-D-Gal-OR where O is an oxygen atom and R is a glycoprotein or glycolipid or H antigen to yield the A determinant α-D-GalNAc-(1,3)-α-L-Fuc-(1,2)-β-D-Gal-OR (Fig. 1). Blood group B individuals express α-(1,3)-galactosyltransferase (GTB; EC 2.4.1.37), which uses the same H-type acceptor structure, but catalyzes the transfer of Gal from UDP-Gal to form the B determinant α-D-Gal-(1,3)-α-L-Fuc-(1,2)-β-D-Gal-OR. Blood group O individuals do not express functional copies of either of the enzymes, and AB individuals express both.

As mentioned above, GTA and GTB are highly homologous enzymes that differ in only four critical amino acids (4, 5). From x-ray diffraction studies it has been suggested that only two of

* The costs of publication of this article were defrayed in part by the payment of page charges. This article must therefore be hereby marked "*advertisement*" in accordance with 18 U.S.C. Section 1734 solely to indicate this fact.
[S] The on-line version of this article (available at http://www.jbc.org) contains supplemental Figs. 1–3 and a supplemental table.
[1] Supported by a European Union Marie Curie fellowship ("Glyco-NMR").
[2] Supported by Deutsche Forschungsgemeinschaft Grants SFB 470 (Project B3) and Me1830. To whom correspondence should be addressed. Tel.: 49-451-500-4230; Fax: 49-451-500-4241; E-mail: thomas.peters@chemie.uni-luebeck.de.

[3] The abbreviations used are: GTA, blood group A α-(1,3)-*N*-acetylgalactosaminyltransferase; GTB, blood group B α-(1,3)-galactosyltransferase; STD, saturation transfer difference; MOPS, 4-morpholinepropanesulfonic acid; UDP-2F-Gal, UDP-2-fluorogalactose.

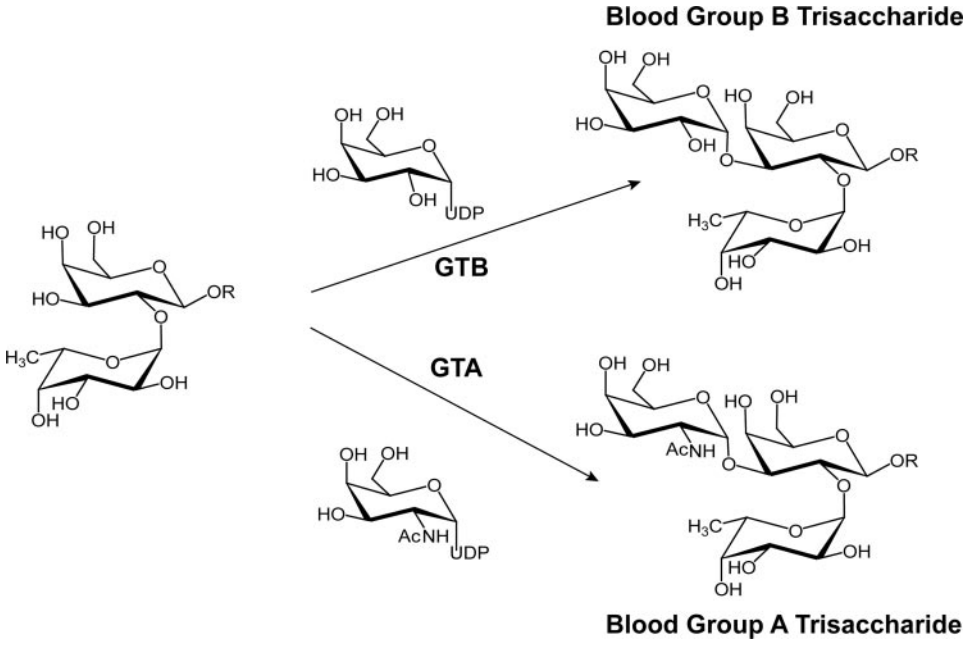

FIGURE 1. **Biosynthesis of blood group A and B antigens from the O(H) precursor.** GTB catalyzes the transfer of Gal from UDP-Gal to the O(H) precursor structure α-L-Fuc-(1,2)-β-D-Gal-OR (where O is an oxygen atom and R is a glycoprotein or glycolipid), whereas GTA transfers GalNAc from UDP-GalNAc to the O(H) precursor.

these amino acids are responsible for the switch in donor specificity, whereas the other two are involved in acceptor binding and turnover (9). To better understand the subtle differences between GTB and GTA, a detailed analysis of enzyme-ligand interactions in aqueous solution is vital. The complex between GTB and UDP is known from the crystal structure, but no data are available for the complex with UDP-Gal, analogs, or fragments of the donor substrate. Therefore, nothing is known yet about the role of the hexopyranose moiety of the donor substrate.

In this study, we have characterized the interactions of a number of different donor ligands with GTB under more physiological conditions, *i.e.* in aqueous solution. We employed saturation transfer difference (STD) NMR (10) to detect and characterize the binding epitopes of these ligands at atomic resolution (10–12). Competitive STD NMR experiments rank the ligands according to their binding affinity, yielding detailed structure-binding relations (13, 14). Therefore, this study provides a key for the design of inhibitors or compounds for directed metabolic engineering with a perspective to be of help for blood transfusions and organ transplantations.

EXPERIMENTAL PROCEDURES

Materials—All ligands except for UDP-2F-Gal, H antigen, and B antigen were obtained from Sigma. UDP-2F-Gal was of synthetic origin.[4] H antigen was chemically synthesized and enzymatically converted to B antigen as described (15).

Expression and Purification of GTB—Recombinant human GTB was expressed in *Escherichia coli* as described previously (15). Cells from a 1-liter culture grown at 30 °C in Terrific Broth medium with M9 supplements were harvested and purified using an SP-Sepharose column and a UDP-hexanolamine-Sepharose column. Fractions with enzymatic activity were pooled; dialyzed against 50 mM MOPS buffer (pH 7.0) containing 100 mM NaCl, 5 mM $MnCl_2$, and 5 mM dithiothreitol; and then stored at −80 °C. Because NMR experiments require deuterated buffers, GTB was dialyzed against water at 4 °C for 1 h (repeated six times) and lyophilized for at least 48 h prior to use. Enzymatic activity was monitored by a radioactive assay (16); protein concentrations were determined with the Bradford assay using bovine γ-globulin as a standard; and purity was controlled by SDS-PAGE analysis. Lyophilized GTB can be stored at −80 °C for several months without a significant loss of activity.

Enzymatic Activity Assays—The dependence of GTB enzymatic activity on the presence of metal ions was determined using a modified version of the method described by Kamath *et al.* (16). In brief, 1 mg/ml bovine serum albumin, 496 μM H disaccharide α-L-Fuc-(1,2)-β-D-Gal-*O*-octyl, 266 μM UDP-Gal, 23 nCi of UDP-[^{14}C]Gal, 0.0727 μg/ml to 0.727 mg/ml lyophilized GTB, and 100 μM to 50 mM $MgCl_2$, $MnCl_2$, or $CaCl_2$ were added to 50 mM MOPS buffer (pH 7.0) to give a final volume of 10 μl. The mixtures were incubated at 37 °C for 20 min, and the reactions were stopped by the addition of 500 μl of ice-cold water. The radiolabeled trisaccharide was isolated from the mixture using Sep-Pak® VacRC C-18 cartridges (Waters Corp.), which were washed with 4 ml of methanol and equilibrated with 4 ml of water prior to use. The reaction mixture was applied to the column and washed with 4 ml of water prior to the elution of the trisaccharide with 4 ml of methanol. Radioactivity was determined by adding 6 ml of Aquasafe 800 (Zinsser Analytic) and counting in a Wallac 1414 WinSpectral scintillation analyzer.

NMR Experiments—STD NMR spectra were obtained at 15 °C using a 12.1-tesla Bruker DRX 500 NMR spectrometer equipped with a triple resonance probehead, incorporating gradients in the *z* axis. Samples contained 20 μM protein and 1–5 mM ligand. The lyophilized protein was resuspended in 50 mM d_{19}-2,2-bis(hydroxymethyl)-2,2′,2″-nitrilotriethanol (pH* 6.7; uncorrected reading for the presence of $^2H^+$), 15 mM d_{10}-1,4-dithio-DL-threitol, and 10 mM $MgCl_2$ and mixed with ligand dissolved in D_2O. For the acquisition of STD NMR spectra, a one-dimensional sequence incorporating a $T_{1\rho}$ filter was used. On-resonance irradiation was performed at 0 ppm, and off-resonance irradiation at 40 ppm. Irradiation was performed using 50 gaussian pulses with a 1% truncation, each with a 49-ms duration and separated by a delay of 1 ms to give a total saturation time of 2 s. The duration of the $T_{1\rho}$ filter was 15 ms. STD NMR spectra were acquired with a total of 1024

[4] M. Palcic and O. Hindsgaul, unpublished data.

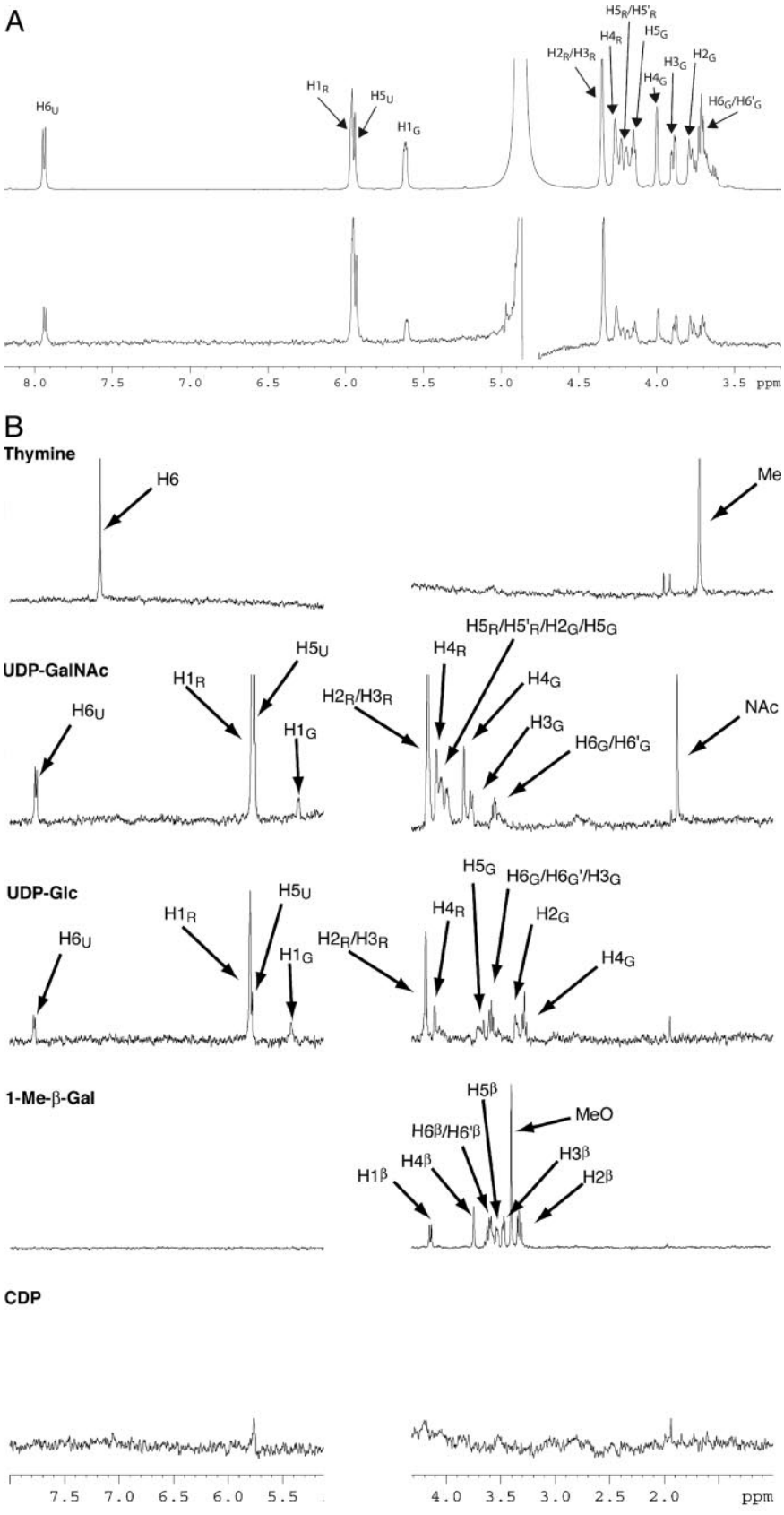

FIGURE 2. *A*, reference (*upper*) and STD NMR (*lower*) spectra of the natural donor substrate UDP-Gal; *B*, STD NMR spectra of different ligands in the presence of GTB. All spectra were measured in the presence of 1 mM ligand with 1024 scans, except methyl β-D-galactopyranoside, which was measured at 5 mM. Assignments in *A* and *B* are shown for signals that are well separated, with *U* denoting the uracil moiety, *R* denoting the ribose moiety, and *G* denoting the galactose or glucose moiety. For all spectra, the scale for chemical shifts is shown at the bottom.

transients in addition to 32 scans to allow the sample to come to equilibrium. Spectra were performed with a sweep width of 5 kHz and 32,768 data points. Reference spectra were acquired using the same conditions, but with only 512 transients. All ligands were assigned under the same conditions as the STD NMR spectra through the use of ^{1}H-^{1}H COSY, ^{1}H-^{1}H total correlation, ^{1}H-^{13}C heteronuclear single quantum correlation, and ^{1}H-^{13}C heteronuclear multiple bond correlation spectra.

To determine the size of the STD effect, the observed signals were integrated with respect to the corresponding signal in the reference spectrum. An STD effect of 100% is therefore defined as when the signals in both spectra have the same intensity. For group epitope mapping, these effects are normalized against the largest STD effect observed. Thus, 100% corresponds to the signal with the largest STD effect.

Titrations to determine relative binding affinities were performed under the conditions described above. Titration STD NMR spectra were obtained in the presence of a second ligand at molar ratios of 0.5, 1, 2, and 4 with respect to the first ligand that was present at 1 mM in all cases. Titration experiments with methyl α-D-galactopyranoside and methyl β-D-galactopyranoside were performed only at a molar ratio of 1:1 of the two ligands. The observed STD signal intensities as a function of the molar ratios revealed the relative binding affinities of the ligands.

For enzyme kinetics, samples with 20 μM protein, 0.5 mM UDP-Gal, and 0.5 mM H antigen were prepared in the presence and absence of metal ions at different concentrations. Each time point consists of a one-dimensional "pulse and acquire" NMR experiment with 16 scans for acquisition and eight dummy scans. The sweep width and recycle delay were the same as for the STD NMR experiments. The decreasing intensities of the well separated signals of H-1_G and H-4_G of UDP-Gal were measured as a

function of reaction time. At the same time, product formation of the corresponding blood group B trisaccharide (Fig. 1) was monitored using the anomeric signals of the trisaccharide.

RESULTS

In another study, we analyzed the binding of UDP-Gal to GTB using transferred nuclear Overhauser effects and STD NMR experiments to determine the bioactive conformation of UDP-Gal in the binding pocket of GTB.[5] Here, we have complemented this work by investigating the binding of UDP-Gal and analogs to GTB using a fragment-based STD NMR approach as applied recently to the binding of substrate ligands to the key enzyme of sialic acid biosynthesis, UDP-GlcNAc 2-epimerase/ManNAc kinase (13, 14). These experiments yield minimum ligand structures ranked according to their binding affinities and thus lead to a comprehensive structure-activity relationship. Such data form a basis for the development of synthetic ligand analogs that may serve as specific inhibitors or that can be useful in metabolic engineering.

NMR Data Reflect the Binding of UDP-Gal and the Activity of the Enzyme—UDP-Gal is the natural donor substrate of GTB and catalyzes the transfer of the galactose residue to H antigen with the release of UDP. The configuration at the anomeric center is retained. Sizeable STD effects were obtained for UDP-Gal in the presence of GTB (Fig. 2*A*). The STD experiments were performed in the absence of any acceptor substrates, demonstrating that UDP-Gal binds to the enzyme also in the absence of H antigen. Furthermore, in the presence of UDP-Gal and H antigen, intensity changes in signals in the ^{1}H NMR spectra reflect conversion to B antigen, showing that the enzyme is active under the NMR conditions. From ^{1}H NMR spectra of a sample of UDP-Gal and H antigen at a concentration of 0.5 mM each and in the presence of 10 mM Mg^{2+}, it is estimated that, after 17 min, 50% of the substrates were converted to products (see Fig. 6*A*). This analysis was based on the well separated signals of H-1 and H-4 of the galactose moiety of UDP-Gal as a function of reaction time. At the same time, product formation was unambiguously shown by the observation of increasing signals, *e.g.* of the anomeric protons of the blood group B trisaccharide. No signals corresponding to D-galactose as a potential product of enzymatic hydrolysis of UDP-Gal were observed, indicating that donor hydrolysis had not occurred as a side reaction.

Epitope Mapping of Ligand Fragments and Ligand Derivatives by STD NMR—STD amplification factors obtained from STD spectra were converted into relative STD effects, with the proton receiving the largest amount of saturation transfer set at 100%. These values reflect the relative amount of saturation transferred from the protein onto the ligand. Therefore, protons with a high STD value are assumed to be in more intimate contact with binding site protons.

First, the binding epitope of UDP-Gal was determined four times with four different protein samples to assess the reliability of the group epitope mapping. The maximum deviation was <7% points. Next, the binding epitope of UDP-Gal was compared with those of the substrate analogs UDP-Glc, UDP-GalNAc, UDP-GlcNAc, and UDP-2F-Gal. The binding epitopes of these analogs were determined based on an average of two or three STD NMR experiments (Fig. 3). It was immediately obvious that, in all cases, the nucleotide moiety received the largest relative amount of saturation transfer and therefore is positioned in the vicinity of protons of the binding pocket. The binding epitope of UDP-Glc was found to be very similar to that of the natural substrate UDP-Gal, with the most prominent differences observed for the protons at C-4 and C-3. UDP-GalNAc and UDP-GlcNAc show the largest differences at C-2 of the sugar moiety. This suggests that UDP-Glc, UDP-GalNAc, and UDP-GlcNAc bind to the same binding pocket, but in different modes or positions compared with the natural substrate UDP-Gal. Furthermore, in the case of UDP-GalNAc and UDP-GlcNAc, the sugar moieties received significantly less overall saturation transfer compared with the sugar moieties of UDP-Gal and UDP-Glc. This indicates that UDP-GalNAc and UDP-GlcNAc have a different overall binding mode compared with UDP-Gal and UDP-Glc. Compared with UDP-Gal, the binding epitope of UDP-2F-Gal shows the largest change for the proton at C-1 of galactose, whereas the STD values observed for H-2 are identical. The overall amount of saturation transferred to the hexopyranose moiety was very similar that observed for UDP-Gal and UDP-Glc. This places UDP-Gal, UDP-2F-Gal, and UDP-Glc in one "binding mode family" as opposed to UDP-GlcNAc and UDP-GalNAc. It should be noted that no hydrolysis was observed in 17 h for any of the ligands.

To explore the individual roles of the nucleotide and sugar moieties in the binding process, additional STD NMR experiments were conducted using fragments of UDP-Gal. STD effects and thus binding to GTB were observed for UDP, UMP, uridine, and uracil. Relative STD values were calculated for all of the ligands (Fig. 4). The resulting binding epitopes of UDP, UMP, uridine, and uracil show a striking similarity, strongly suggesting that all ligand fragments bind in a similar manner. The epitopes are very similar to those of the nucleotide moiety in UDP-Gal, indicating that they all bind to the same site. Small differences may arise because of a slightly different binding mode in the absence of the sugar moiety.

Finally, we performed STD NMR experiments with the sugar derivatives α-D-galactose 1-phosphate, α-D-galactose, β-D-galactose, methyl α-D-galactopyranoside, methyl β-D-galactopyranoside, and ribose to probe their roles in GTB binding. To learn about the structural requirements of the base, we also studied CDP, CMP-Neu5Ac, ADP, GMP, and thymine as ligands. Of these ligands, only D-galactose, the corresponding methyl galactopyranosides, and thymine led to significant STD signals. α-D-Galactose 1-phosphate, CDP, ADP, and GMP delivered extremely weak STD responses that made quantification impossible, indicating that these ligands are essentially outside the range of binding affinities covered by STD NMR (usually a K_D between ~1 nM and 10 mM). The STD spectra of selected ligands in comparison with that of the natural donor ligand are shown in Fig. 2*B*. The corresponding binding epitopes are summarized in Fig. 4. Different binding epitopes were observed for α-D-galactose and β-D-galactose. The bind-

[5] Angulo, J., Langpap, B., Blume, A., Biet, T., Meyer, B., Krishna, N. R., Peters, H., Palcic, M. M., and Peters, T. (2006) *J. Am. Chem. Soc.*, in press.

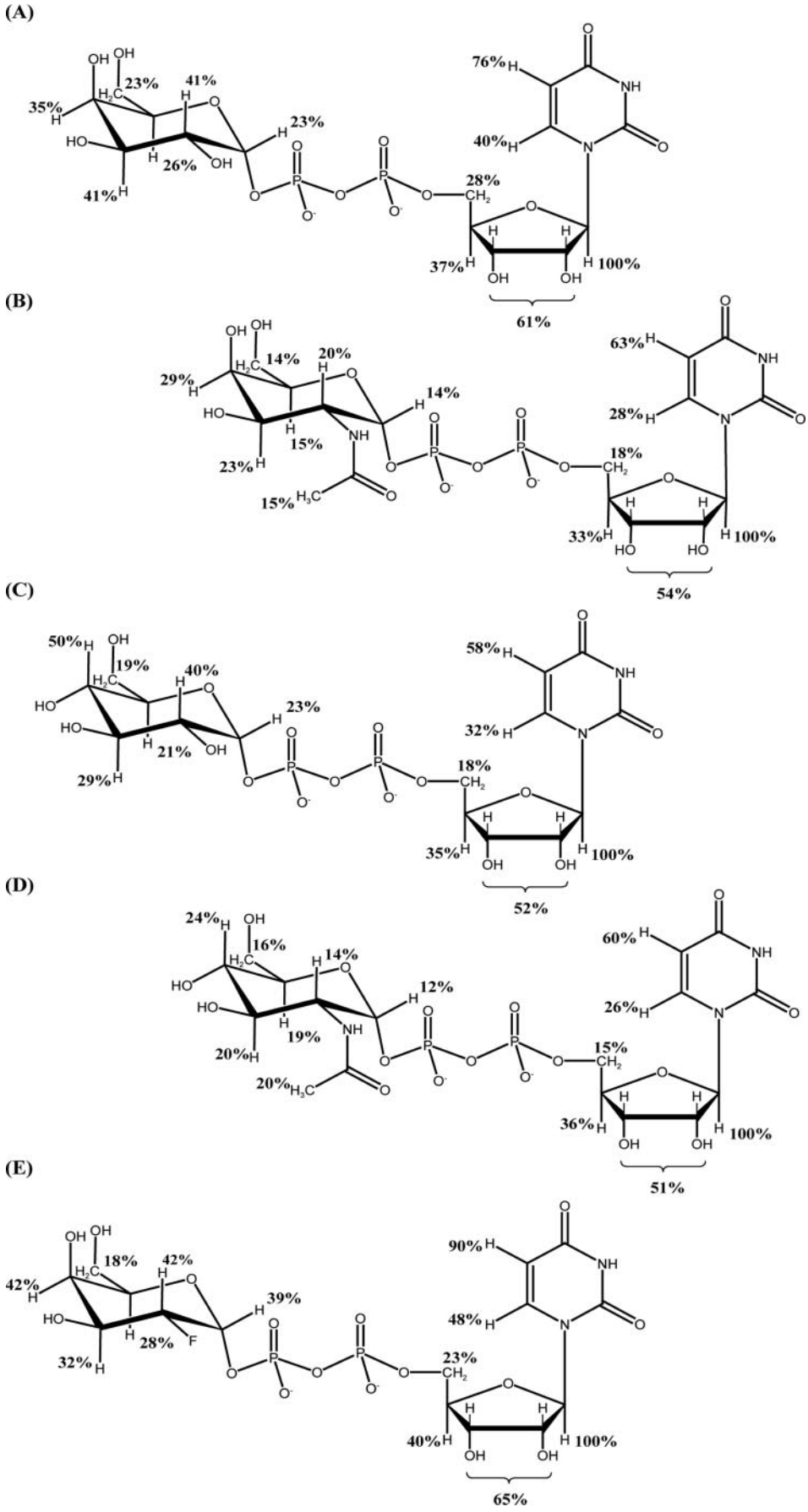

ing epitopes of the methyl glycosides are identical to those of the respective reducing anomers of galactose. Because the natural donor UDP-Gal contains an α-D-galactose moiety and the acceptor H antigen contains a β-D-galactose residue, it is reasonable to hypothesize that α-D-galactose binds to the donor site, whereas β-D-galactose binds to the acceptor site. It is interesting to note that uracil and thymine have different binding epitopes, which may suggest a different binding mode.

STD NMR Titrations—To obtain the relative binding affinities of the fragments and to relate them to the natural donor substrate UDP-Gal, we performed competitive STD titrations. Up to five data points were recorded per titration, and a quantitative analysis of relative K_D values was performed for some of the ligands according to protocols published previously (11, 18). For competitive STD titrations, one identifies signals of the two potentially competing ligands that show no signal overlap. One ligand is then held at a constant concentration, whereas the second ligand is titrated into the solution of the first ligand in the presence of GTB. Here, we measured the decay of STD signal intensity of the first ligand, *i.e.* the ligand at constant concentration. Qualitatively, one can estimate whether a second ligand is a better binder from one experiment in which both ligands are present at a known concentration. For example, if the STD signal decreases by >50% when both ligands are present at the same concentration, the second ligand is considered to be a better binder. For a quantitative analysis, a number of titration points have to be recorded, and relative STD intensities (I_{STD}) have to be determined as a function of the total concentration of the inhibitor (I_0) and the total concentration of the ligand (L_0). The ligand that is kept at a constant concentration is characterized by the dissociation constant K_D, and the ligand that is titrated and is therefore present at varying concentrations is assigned a second dissociation constant (K_I). One of the two dissociation constants, K_I or K_D, has to be known to derive the other constant via a nonlinear least squares fit to the following equation (18, 19): $I_{STD} = -100 \times ((K_D/L_0) \times (I_0/K_I))/(1 + (K_D/L_0) \times ((1+ I_0/K_I))) + 100$.

To derive relative K_D values from competitive titrations for a row of compounds, one needs an independent reference value. We have assumed that the K_{ib} value of 17 μM published for UDP-Gal (20) is a good approximation for the dissociation constant K_D. In this study, we employed up to five titration points to derive a ranking of the dissociation constants of UDP-Gal and derivatives thereof. The complete set of fitted data is found in the supplemental material and suggests that a precise quantitative ranking will require significantly more data points to be acquired. Nevertheless, our data are of sufficient quality to provide a semiquantitative ranking of binding affinities as summarized in Fig. 5. For nucleotides and smaller fragments, relative affinities have been estimated qualitatively only because a precise determination of K_D values would require the acquisition of significantly more titration points, which is the subject of current experimental work in our laboratory that aims at the elucidation of a complete set of thermodynamic parameters for the binding reactions in question.

Competitive binding was observed between all ligands. This indicates that all ligands examined bind to the same site. UDP turned out to be the best binder, with a K_D of ~5–15 μM (Fig. 5*A*). UDP-Gal, UDP-Glc, and UMP all displayed lower binding affinities for GTB compared with UDP, with their K_D values ranging between 10 and 20 μM. The insertion of an *N*-acetyl group at the 2-position of the hexopyranose further reduced the binding affinity (Fig. 5*A*), and a K_D of only ~60 μM was observed. As already mentioned, very weak STD signals were obtained for CDP, ADP, GMP, and α-D-galactose 1-phosphate, indicating that binding was either very weak or very strong. By performing competitive titrations, it was unambiguously shown that these ligands were displaced from the binding site upon the addition of UDP. This shows that their binding affinities are much lower compared with UDP and that the ligands bind to the same site as UDP. Furthermore, titration experiments with UDP showed that thymine also binds to the donor-binding site with a binding affinity in the same range as uracil.

To test the hypothesis that the α- and β-anomers of D-galactose bind to the donor or acceptor site, respectively, competitive titrations with UDP-Gal and the H disaccharide α-L-Fuc-(1,2)-β-D-Gal-*O*-octyl were performed. To exclude "mixing" of the STD effects from the two anomers due to mutarotation, competitive titrations were performed using methyl α-D-galactoside and methyl β-D-galactoside, which were shown to have the same binding epitopes as α- and β-galactose. The titrations showed that there was strong competition between methyl β-D-galactoside and the acceptor disaccharide, but at the same time, it was observed that UDP-Gal also displaced methyl β-D-galactoside from the binding site to a certain extent. Therefore, methyl β-D-galactoside binds to both sites, the donor and acceptor sites, and consequently, the observed binding epitope represents an average of the binding to the acceptor and donor sites. Interestingly, methyl α-D-galactoside STD signals showed almost no change in intensity upon the addition of UDP-Gal, and the addition of the H or B trisaccharide led to a slight signal reduction only. As both the donor and acceptor ligands cannot efficiently displace methyl α-D-galactoside from binding, there must be a third binding site with α-D-galactose specificity.

Dependence of GTB Activity on Metal Ions—For many glycosyltransferases, it is known that Mn^{2+} is essential for the enzyme reaction to proceed. For GTB, enzymatic activity persisted even in the presence of EDTA (Fig. 6, *A* and *B*). The influence of metal ions on the enzymatic activity of GTB was examined by straightforward one-dimensional ^{1}H NMR experiments under conditions also applied for the STD NMR experiments, *i.e.* the concentration of GTB was 20 μM. The presence of 100 μM $MnCl_2$, $MgCl_2$, or $CaCl_2$ in the sample caused a significant increase in enzymatic activity compared with the

FIGURE 3. **Binding epitopes as determined by group epitope mapping from ^{1}H STD NMR spectra: UDP-Gal (*A*), UDP-GalNAc (*B*), UDP-Glc (*C*), UDP-GlcNAc (*D*), and UDP-2F-Gal (*E*).** Relative STD effects were calculated from STD amplification factors (*cf.* "Experimental Procedures"). Values are the means of an average of two to four experiments with a S.D. of a maximum of 7% points of the relative STD amplification factors (11). All ligands show very similar binding epitopes, suggesting that they all bind to the same binding pocket and in the same binding mode. In all cases, the nucleoside moiety received the largest relative saturation transfer and therefore is in the most intimate contact with protons in the binding site.

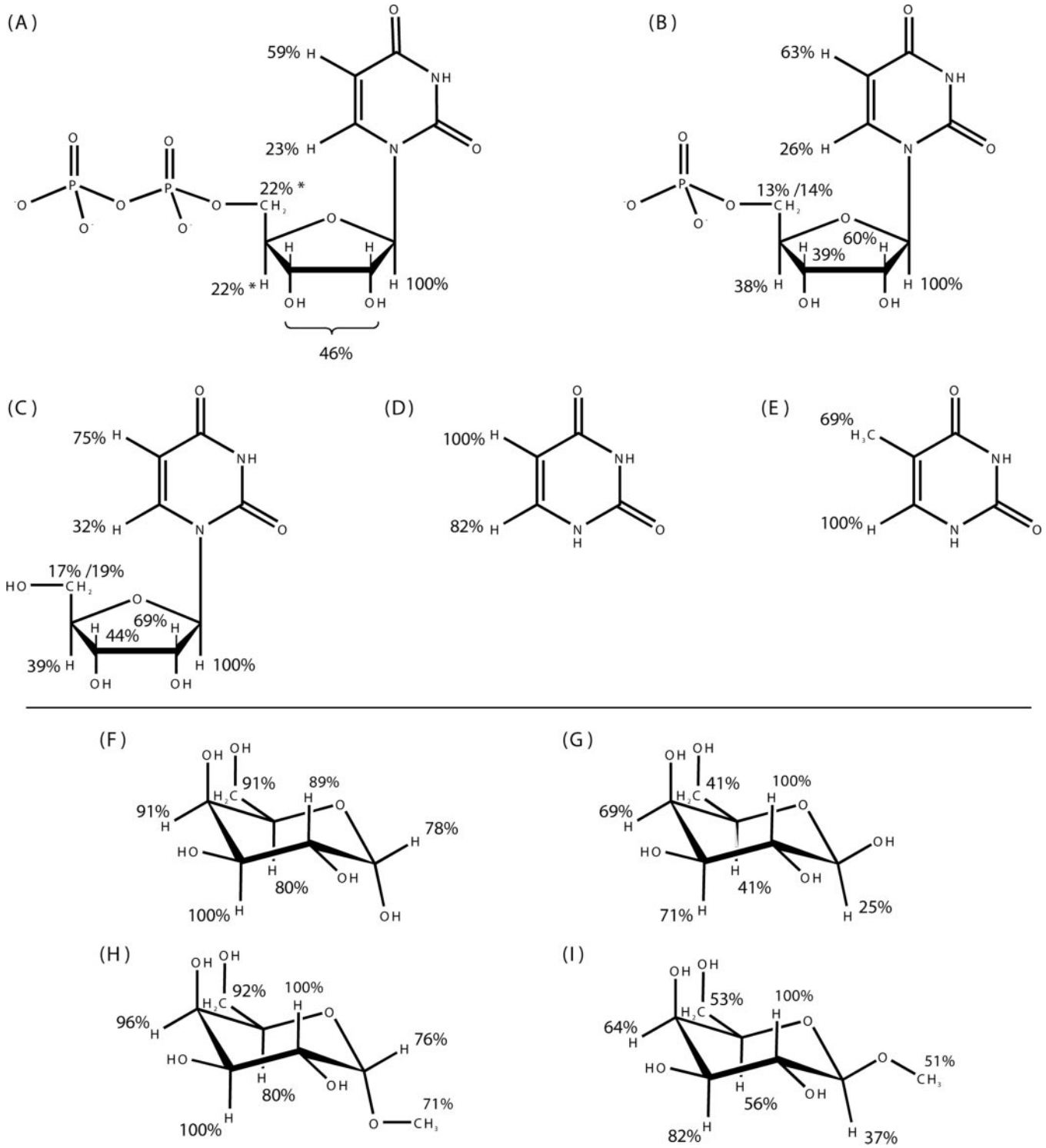

FIGURE 4. **Binding epitopes from ^{1}H STD NMR experiments: UDP (*A*), UMP (*B*), uridine (*C*), uracil (*D*), thymine (*E*), α-D-galactose (*F*), β-D-galactose (*G*), methyl α-D-galactopyranoside (*H*), and methyl β-D-galactopyranoside (*I*).** All nucleoside derivatives show very similar binding epitopes (*cf.* Fig. 3), except for thymine. In the case of α/β-D-galactose and methyl α/β-D-galactopyranoside, values are the means of an average of three experiments with average S.D. values of 13 and 4% points, respectively. The α-anomers (*F* and *H*) and the β-anomers (*G* and *I*) show rather similar binding epitopes, suggesting that they bind to the same binding pocket and in the same binding mode. On the other hand, α- and β-anomers show different binding epitopes, indicating that they bind to different binding sites. *Asterisks* denote signal overlap.

absence of divalent metal ions (see supplemental material). For example, 8 h were required for 50% transfer of UDP-Gal to H antigen in the presence of EDTA, whereas in the presence of 100 μM Mn^{2+}, Mg^{2+}, or Ca^{2+}, 50% of the reaction was completed in ~3 h. An even more significant acceleration was observed at higher metal ion concentrations of 10 mM, as shown for Ca^{2+} and Mg^{2+} ions (Fig. 6*A*). Because of severe paramagnetic line broadening, NMR measurements are not possible at

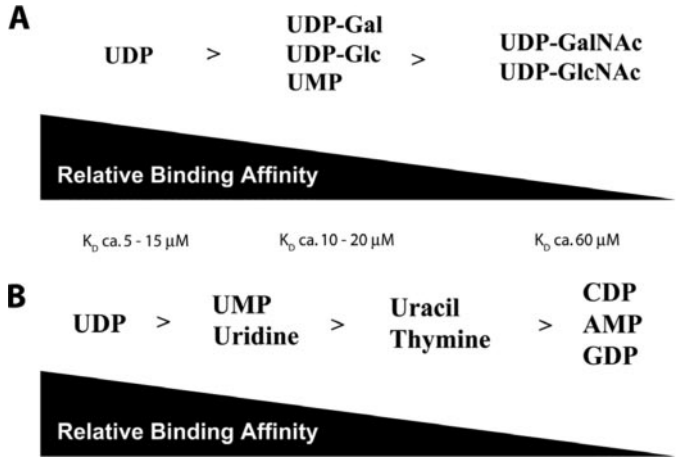

FIGURE 5. **Relative binding affinities of UDP-Gal and derivatives.** Competitive STD NMR titrations (11, 13, 14) showed that all these ligands competed with each other and therefore bind to the same binding site. The K_D values given in *A* are estimates based on the data in the supplemental table. For the calculations in the supplemental table, a K_D of 17 μM was assumed for UDP-Gal (20). This value was derived from enzyme kinetic experiments, and the true K_D value may be slightly different. A precise quantification of K_D values would require a much larger number of data points from the titrations. Therefore, the values in *A* assume a more generous error margin. Nevertheless, the analysis allows a qualitative ranking of the binding affinities of the ligands.

concentrations of Mn^{2+} higher than ~100 μM (*cf.* supplemental material for activity measurements at metal ion concentrations of 100 μM). In the presence of 10 mM Mg^{2+} or Ca^{2+} (Fig. 6*A*), the conditions used for STD NMR, only 17 min were required for the transfer to be 50% complete.

Interestingly, under NMR conditions in which the enzyme concentration was 20 μM, no differences in the transfer rates were detected for Mn^{2+}, Mg^{2+}, or Ca^{2+} at a concentration of 100 μM. Because previous studies on the closely related enzyme GTA reported increases in activity for Mn^{2+} compared with Mg^{2+} or Ca^{2+} (21), these results were unexpected. Therefore, additional radiochemical assays were performed to substantiate the NMR data. In general, it was confirmed that GTB is active at a low level (50–100 dpm) (*cf.* Fig. 7*A*) even in the presence of 2 mM EDTA, indicating that trace amounts of bivalent metal ions are sufficient to allow catalysis or that the enzyme is active even in the absence of metal ions. Nevertheless, an increase in metal ion concentration promotes enzymatic activity. The activity increase observed in the radiochemical assays in the presence of Mg^{2+} or Ca^{2+} was comparable to that observed by NMR (Fig. 7*A*). In contrast to the NMR experiments, under the conditions of the radiochemical assay, a pronounced increase in GTB activity was observed in the presence of Mn^{2+} compared with Mg^{2+} and Ca^{2+} at both high (10 mM) and low (100 μM) concentrations.

To explain this remarkable increase in enzymatic activity in the presence of Mn^{2+} in the radiochemical assays but not in the NMR assays, we performed additional radiochemical assays at different concentrations of GTB because this was the main difference between the NMR and radiochemical assay conditions. We varied the protein concentration over a range of 2 nM to 20 μM in the presence of either 100 μM or 10 mM metal cation. A plot of the relative increase in the enzymatic activity by metal ions as a function of the protein concentration revealed that the same curves were obtained for both metal ion concentrations,

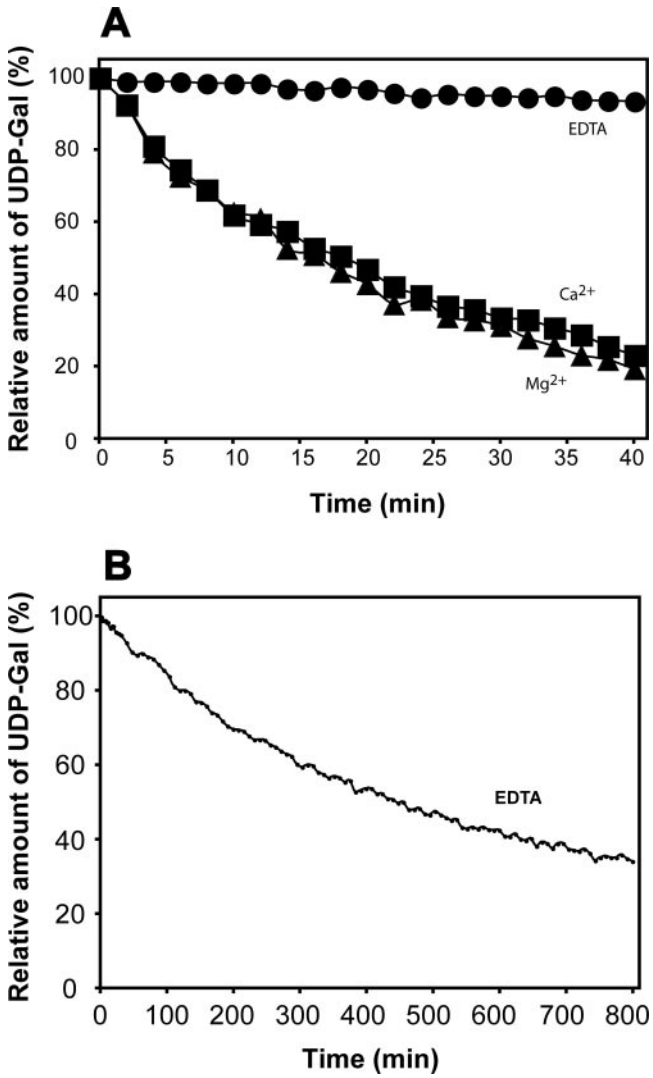

FIGURE 6. *A*, averaged intensity change in the ^1H NMR signals of H-1_G and H-4_G of UDP-Gal in the presence of H antigen and GTB as a function of time. ●, data obtained in the absence of bivalent metal ions and in the presence of 1 mM EDTA; ▲, data obtained in the presence of 10 mM Mg^{2+}; ■, data obtained in the presence of 10 mM Ca^{2+}. The curves for Mn^{2+} are not shown because paramagnetic line broadening prevents any intensity measurement at this concentration. For a corresponding graph that includes also data points for Mn^{2+} at a lower metal ion concentration of 100 μM, see supplemental Fig. 2. *B*, extension of the data in *A* (obtained in the presence of 1 mM EDTA over a period of 13.5 h) showing that the enzyme is active under these conditions. The ^1H NMR signals of free galactose were not observed, indicating that no hydrolysis of the donor substrate occurred during the measurements.

although the absolute increase in activity was higher in the case of 10 mM metal ion. More interestingly, these data show that Mn^{2+} significantly promoted enzymatic activity compared with Mg^{2+} or Ca^{2+} only at GTB concentrations lower than ~3 μM (Fig. 7*B*). The increase in enzymatic activity plotted against the protein/metal concentration ratio shows that this ratio had no significant influence on the relative activity increase in the presence of different metal cations, and consequently, the curves for 100 μM and 10 mM metal ion look almost identical, except for a shift by a factor of 100 (see supplemental material).

Therefore, the critical aspect of the relative increase in enzymatic activity due to different metal ions is neither the protein/metal concentration ratio nor the absolute metal ion concen-

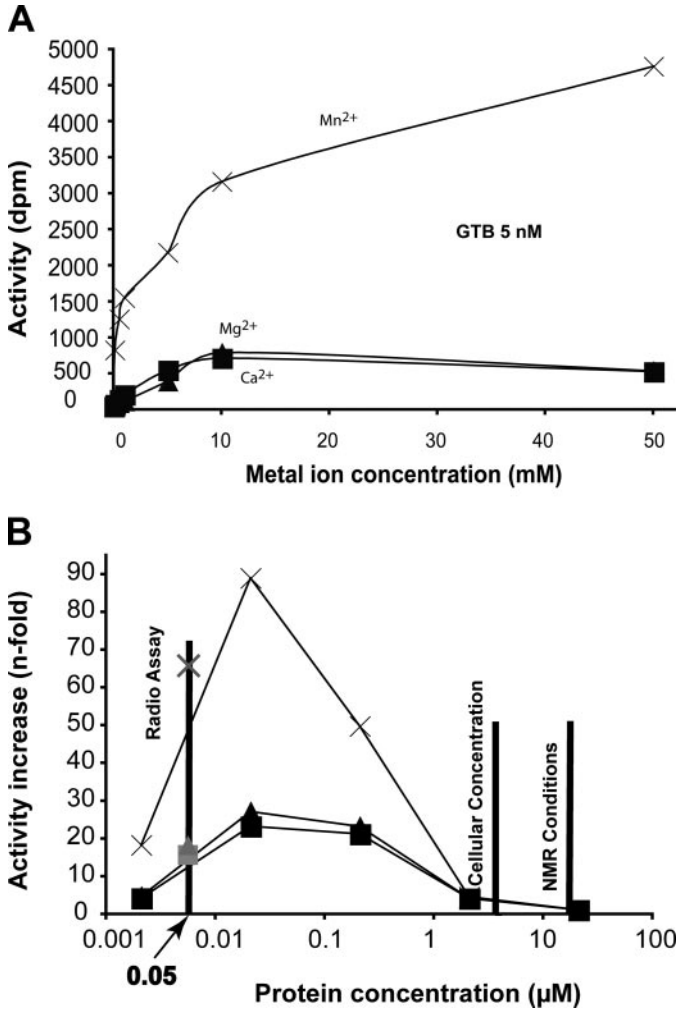

FIGURE 7. *A*, GTB activity in the presence of different $MgCl_2$, $CaCl_2$, and $MnCl_2$ concentrations. Enzymatic activity was measured in a radiochemical assay with a protein concentration of 5 nM. EDTA (2 mM)-treated samples displayed base activities between 50 and 100 dpm. ▲, data obtained in the presence of different Mg^{2+} concentrations; ■, data obtained in the presence of different Ca^{2+} concentrations; ×, data obtained in the presence of different Mn^{2+} concentrations. Mn^{2+} significantly increased activity compared with Mg^{2+} or Ca^{2+}, even with only 100 μM metal cation present. *B*, increase in GTB activity relative to samples containing 2 mM EDTA with no bivalent metal ions added. Activities were determined at different protein concentrations in the presence of 10 mM $MgCl_2$, $CaCl_2$, or 10 mM $MnCl_2$. Enzymatic activity was measured using a radiochemical assay as described for *A*. ▲, data obtained in the presence of Mg^{2+}; ■, data obtained in the presence of Ca^{2+}; ×, data obtained in the presence of Mn^{2+}. The same curves were obtained in the presence of 100 μM metal cation instead of 10 mM (*cf.* supplemental Fig. 3). In both cases, the bivalent metal ions significantly promoted GTB activity only at protein concentrations less than ~3 μM. The scale for the protein concentration is logarithmic to display the large range of GTB concentrations applied. *Bars* indicate typical protein concentrations used for a standard radioactivity assay as performed in *A*, found inside the cell, and used for the STD NMR experiments in this study. The cellular concentration of GTB was estimated according to simple assumptions as discussed under "Discussion." It should be noted that the true concentrations of GTB in the Golgi membrane may be different. The data points from the activity assay performed in *A* at 5 nM GTB are included in *B* (Radio Assay) to emphasize the reproducibility of the data.

tration, but rather the protein concentration itself (Fig. 7*B*). In additional control experiments, radiochemical assays were also conducted in the absence of bovine serum albumin, and the results described above were confirmed. However, the absence of bovine serum albumin decreased the overall enzymatic activity by ~50%.

DISCUSSION

Binding epitope analysis of UDP-Gal and its derivatives bound to human blood group B galactosyltransferase unambiguously revealed that the nucleotide moiety dominates the binding of donor substrate ligands. In all cases, H-1′ of the ribose ring and H-5 of the uridine ring received the largest amount of saturation transfer. Similar binding modes were previously inferred from STD NMR experiments for UDP-Gal binding to the inverting β-1,4-galactosyltransferase T1 (22) and for UDP-GlcNAc binding to UDP-GlcNAc 2-epimerase (13). It is conjectured that the base directs the ligands into the binding pockets of these enzymes. In accordance with this observation, crystal structure data show that the uracil ring has stacking interactions with aromatic amino acid side chains that form a recognition site for the base. The crystal structure of UDP-Gal bound to the inverting glycosyltransferase β-1,4-galactosyltransferase T1 (23) shows that, in this case, the uracil ring of UDP interacts with the side chains of Arg^{191} and Phe^{266}. Crystal structure data for bovine α-1,3-galactosyltransferase, a retaining glycosyltransferase closely related to GTB, also reveal stacking interactions of the uracil ring with the hydrophobic amino acids Phe^{134} and Val^{136} (24–26). The crystal structure of the retaining GTB complexed with UDP reveals a stacking interaction between Tyr^{126} and the uracil ring (9). In this structure, Ala^{177}–Cys^{196} and the Lys^{346}–Pro^{354} (C terminus) are not visible because they are disordered. As it is likely that these amino acids are required to close the enzyme donor substrate-binding pocket, we also inspected the homology model that had been generated for GTB prior to the publication of the x-ray structure (27). The model suggests a stacking of the uracil ring with two amino acid side chains, *viz.* Tyr^{126} and Val^{184}. This closely parallels the situation in β-1,4-galactosyltransferase T1 and α-1,3-galactosyltransferase.

The observations that the gross binding epitopes of UDP-Gal, UDP-Glc, UDP-GalNAc, and UDP-GlcNAc are rather similar and that binding is also observed for UDP, UMP, uridine, and uracil support the hypothesis that UDP guides the ligand into the donor-binding site of GTB. In accordance with this hypothesis, all ligands compete with each other for binding, indicating that they all bind to the same (donor) site. Competitive titrations conducted with UDP-Gal, UDP-Glc, and UDP revealed that the binding process is controlled by the UDP moiety. This implies that the galactose residue has a minor influence on the free energy of binding.

The fact that UDP-Gal and UDP-Glc have similar binding epitopes and very similar binding affinities for GTB suggests that the enzyme cannot discriminate between the two ligands. In terms of binding affinity, this is true, but in terms of enzymatic activity, it was shown that the transfer rate of UDP-Glc (k_{cat}) is only 0.01% compared with that of UDP-Gal (28). Therefore, we suggest a model in which the sugar moiety determines the specificity of the enzyme reaction, but not of the binding, whereas the nucleotide is responsible for the affinity of the ligand. It is proposed that, upon binding the donor ligand, the rather flexible sugar residue is trapped in a bound conformation,[5] leading to a substantial loss of conformational entropy. If this is not sufficiently compensated for by the enthalpy of bind-

ing of a hexopyranose ring, this would explain the slightly better binding affinity of UDP compared with those of UDP-Gal and UDP-Glc. A microcalorimetric analysis of the binding of UDP, UDP-Gal, and UDP-Glc to α-1,3-galactosyltransferase has been performed (26). In that case, unlike in our study, the binding affinity of UDP-Gal (K_D = 60 μM) was significantly better than of UDP-Glc (K_D = 258 μM), whereas in accordance with our observations, UDP was the best binder (K_D = 53 μM). An entropy-enthalpy compensation as suggested above was not observed. We are currently performing a systematic combined STD NMR and surface plasmon resonance-based approach to obtain more detailed thermodynamic data.

In another study, we performed a thorough quantitative analysis of the bound conformations of UDP-Gal and UDP-Glc based on transferred nuclear Overhauser effect experiments and STD NMR build-up curves employing full relaxation and exchange matrix simulations.[5] Based on this quantitative analysis, we proposed a mechanism that accounts for the importance of the OH-4 group of galactose for the propagation of the glycosyl transfer reaction.[5] We suggested that the side chains of Asp^{302} and Glu^{303} act like tweezers that lock the galactose (but not the glucose) residue such that a nucleophilic attack at the anomeric center is successful.

The binding epitopes observed for UDP-GalNAc and UDP-GlcNAc differ from those for UDP-Gal and UDP-Glc with respect to the hexopyranose moieties. From docking models based on the homology model of GTB (data not shown), steric conflicts with the bulky *N*-acetyl groups force the hexopyranose rings into different orientations in the binding pocket. Apparently, in the case of UDP-GalNAc, there is still a favorable orientation of the OH-4 the sugar ring relative to the Glu^{303} side chain to facilitate the nucleophilic attack. Therefore, the k_{cat} for UDP-GalNAc is still 6–8% compared with that for UDP-Gal (15, 29). In the case of UDP-GlcNAc, no transfer was observed (20). The bulky *N*-acetyl group and the "wrong" stereochemistry at C-4 add up and preclude any measurable enzymatic activity. Steric conflicts are also responsible for the reduction of binding affinity as observed in competitive STD titration experiments.

Interestingly, the cellular concentration of UDP-Glc is 3.5-fold higher than that of UDP-Gal in normal rat liver cells (30). Taking into account that GTB has the same binding affinity for UDP-Glc as its natural substrate UDP-Gal, the question arises as to whether GTB can be reversibly inhibited by UDP-Glc under physiological conditions. In fact, the answer to this question depends on how effectively UDP-Glc is transported across the Golgi membrane into the lumen of the Golgi apparatus. Nucleotide sugars are subject to active transport by antiporters in the Golgi membrane, as has been summarized in a recent review (31). For the plant *Arabidopsis thaliana*, it has been observed that the UDP-Gal transporter also transports UDP-Glc (32). Moreover, it has been shown recently that multisubstrate-specific nucleotide sugar transporters occur in human cells (33). This makes it very difficult to estimate the "true" UDP-Gal and UDP-Glc concentrations in the Golgi. If UDP-Glc were transported as efficiently as UDP-Gal, it could inhibit human blood group B galactosyltransferase.

The cellular concentration of UDP-GalNAc is in the same range as that of UDP-Gal, whereas the concentration of UDP-GlcNAc is twice that of UDP-Gal. GTB has a lower affinity for UDP-GalNAc and UDP-GlcNAc than for the natural substrate UDP-Gal (*cf.* Fig. 5). Whether these nucleotide sugars function as inhibitors again depends on their concentration in the Golgi, which is in turn regulated by respective nucleotide sugar transporters. Therefore, it is very difficult to draw firm conclusions about the potential inhibitory role of these activated sugars until their intra-Golgi concentrations are known.

UDP is released as a by-product of many glycosyltransferase reactions and displays a higher binding affinity for GTB compared with UDP-Gal. It is known that UDP is effectively cleaved by nucleotide diphosphatases (34), and the resulting UMP is then transported into the cytosol by antiporters, which transport UDP-activated sugars into the lumen of the Golgi (31). Therefore, despite the high binding affinity of UDP for GTB, it is unclear whether UDP is a strong competitive inhibitor *in vivo*.

The fragment-based approach further showed that the affinity of GTB for a specific donor-type ligand critically depends on the presence of the β-phosphate and ribose moieties. Accordingly, the binding affinity of UMP is significantly reduced compared with that of UDP, and the affinity of uracil is further reduced relative to that of uridine. Interestingly, one phosphate residue is sufficient to direct α-D-galactose 1-phosphate into the donor site, resulting in weak STD signals. In contrast, for α-D-galactose, no significant binding to the donor site was detected. Similar results were found previously when studying ligand binding to rat UDP-GlcNAc 2-epimerase (13). In that case, UMP was the minimum fragment with binding activity, and smaller fragments such as uridine led to no significant interactions with the enzyme (35). In contrast to those previous findings, in the case of GTB, binding of uridine and even uracil was observed. Therefore, it is speculated that the UDP-binding pockets of the epimerase and GTB are significantly different.

Our experiments show that uracil is the minimum structural fragment that binds to GTB, whereas the ribose moiety alone has no binding affinity. On the other hand, the addition of the ribose and β-phosphate moieties increased the binding affinity for GTB. It is known that the β-phosphate moiety is recognized by the D*X*D motif (9). Therefore, the uracil ring may be considered as a "molecular anchor" that guides donor-type ligands into the donor-binding site (Fig. 8).

The observation that CDP, as well as AMP and GDP, is an extremely weak binder compared with UDP underscores the importance of uracil as a molecular anchor. In a cell, the activated nucleotide sugar substrates UDP-Glc, UDP-GlcNAc, UDP-Gal, UDP-GalNAc, GDP-Fuc, GDP-Man, and CMP-Neu5Ac presumably are present at the same time and in the same compartments of the cell. Therefore, the corresponding glycosyltransferases must be able to distinguish between the different activated sugars. Our experiments revealed the details of this discrimination process for GTB, which is based, in the first place, on the recognition of uracil and, in the second place, on a "kinetic" discrimination of the pyranose moiety. It is notable that GTB does not discriminate between thymine and uracil. But because there is no known thymine-activated sugar in a

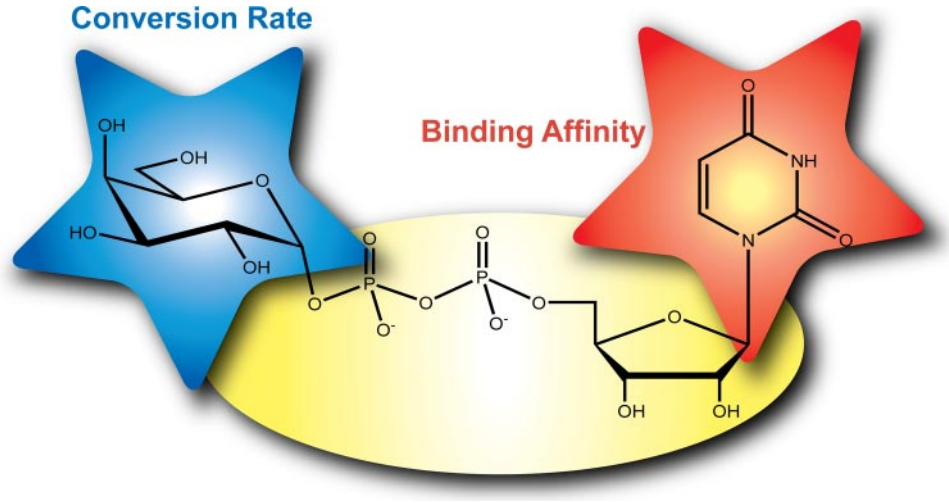

FIGURE 8. **Representation of UDP-Gal displaying the contributions of each moiety to molecular recognition and enzymatic activity.** The uracil moiety (*red*) serves as a molecular anchor, as the enzyme distinguishes its donor substrate UDP-Gal on the basis of the base. The ribose ring and diphosphate bridge (*yellow*) improve the binding affinity, whereas the galactose residue (*blue*) does not contribute to the free energy of binding, but rather tunes the enzymatic activity.

cell, there has never been any requirement for this kind of differentiation.

Our experiments showed that β-galactose binds slightly better to the donor-binding site of GTB than does α-galactose. We suggest that the equatorial hydroxyl group at C-1 of β-galactose is able to substitute for the oxygen of the β-phosphate of UDP-Gal, thus rendering β-galactose a better binder, yet a large proportion of β-galactose binds to the H antigen site, which is known to recognize β-galactose as part of the H antigen acceptor. The observation that α-galactose binding can be inhibited by the addition of neither donor substrate nor acceptor ligand may be explained by the presence of a third binding site for α-galactose. Further experiments will be required to validate this hypothesis.

Several glycosyltransferases are thought to require Mn^{2+} as an essential cation for their enzymatic activity. Here, we have shown that, in contrast to the current perception, GTB retains activity even in the virtual absence of any divalent metal ions. Because even high concentrations of EDTA cannot entirely eliminate metal ions, it remains an open question as to whether the residual activity is due to traces of metal cations or whether it reflects a "base activity" of the enzyme in the absence of any metal cations. For other glycosyltransferases, *e.g.* bovine β-1,4-galactosyltransferase, a much more stringent dependence on the presence and type of metal cations has been described (36–38).

Nevertheless, the addition of metal ions causes a concentration-dependent increase in GTB activity. Our experimental results raise the question as to whether Mn^{2+} functions as the natural cofactor of GTB under physiological conditions. It has been suggested recently that Zn^{2+} may function as the natural cofactor instead of Mn^{2+} for the related α-1,3-galactosyltransferase (39). For the NMR experiments described here, we excluded Zn^{2+} because the stability of UDP-Gal in its presence is significantly reduced compared with that in the presence of Mg^{2+}, Mn^{2+}, or Ca^{2+}. In the presence of Zn^{2+}, UDP-Gal is essentially completely hydrolyzed after 50 h at 25 °C, whereas <8% hydrolysis is observed in the presence of Mg^{2+}.[6]

Another surprising finding is that the modulation of GTB activity by metal cations depends on the absolute concentration of GTB (*cf.* Fig. 7*B*). At protein concentrations higher than ~3 μM, the addition of bivalent metal cations to the buffer resulted in a mere ~3-fold increase in enzymatic activity. At these protein concentrations, no difference in the effects of the bivalent cations Mn^{2+}, Mg^{2+}, and Ca^{2+} was observed in the NMR and radiochemical assays. But interestingly, at protein concentrations lower than ~3 μM, Mn^{2+} increased GTB activity more significantly compared with the other metal ions. At present, the reasons for this surprising dependence of the relative rate constants on the absolute protein concentration and not on the metal ion concentrations or the protein/metal ion ratio remain unclear. Recent NMR experiments with ^{2}H,^{15}N-labeled GTB and dynamic light scattering experiments performed in our laboratory,[7] suggest that the conformational and oligomeric state of the enzyme is concentration- and temperature-dependent. These experiments may deliver explanations for the effects observed.

In this context, it is also surprising that the increase in the reaction rate upon the addition of bivalent metal ions was more pronounced in the NMR-based assay (Fig. 6, *A* and *B*) than in the radiochemical assay (Fig. 7, *A* and *B*). The plots indicate an ~28-fold larger reaction rate in the presence of Mg^{2+} or Ca^{2+}. On the other hand, the data from the radiochemical assay indicate only a 2–3-fold increase in the reaction rate. The different temperatures at which the assays were performed (NMR-based assay at 15 °C and radiochemical assay at 37 °C) can only partly account for this discrepancy. But besides the temperature, there are other experimental boundary conditions that are different for the NMR-based assay *versus* the radiochemical assay such as the absence of bovine serum albumin in the NMR-based assay. It should also be noted that, at higher enzyme concentrations such as those used in the NMR experiments or as found under *in vivo* conditions, a quasi-steady-state assumption cannot be made. A more complex theory reflects rate laws under *in vivo* conditions and at high enzyme concentrations (40, 41). Therefore, the different donor and acceptor concentrations used in the assays may have also contributed to the effect observed. Interestingly, at a lower metal ion concentration of 100 μM (*cf.* supplemental Fig. 2), the results from the NMR-based assay matched those from the radiochemical assay very well. As indicated above, we cannot explain this discrepancy at

[6] T. Biet and T. Peters, unpublished data.
[7] H. Peters, J. Angulo, and T. Peters, unpublished data.

the moment. A complete and systematic kinetic analysis using both assay formats will be required to resolve this problem. It will also be necessary to link these results to prospective NMR data on the conformational behavior of GTB.

As GTB transfers terminal sugars, the enzyme should be located in the *trans*-Golgi. It is known that, in highly active secretory cells, ~20% of the cell volume is made up by the endomembrane system (42, 43). One may further assume that about one-twentieth of the endomembrane system constitutes the *trans*-Golgi compartment. It has been reported that 200 μg of purified GTA can be isolated from 1 kg of porcine submaxillary glands (44) with a loss of 87%, so there are ~1500 μg of GTA in 1 kg of submaxillary glands. Taking into account that 20% of the submaxillary gland cells constitute the endomembrane system and that one-twentieth of this is *trans*-Golgi, this results in 10 g of *trans*-Golgi/1 kg of submaxillary glands. This in turn means that 1500 μg of GTA are found in 10 g of *trans*-Golgi. This crude estimation shows that the concentration of GTB in a cell is at least 150 μg/ml, corresponding to a concentration of 4 μM. Therefore, the NMR conditions with protein concentrations in this range should be much closer to the physiological conditions in a cell than the standard radiochemical assay conditions used routinely for Michaelis-Menten kinetics, where a drastic activity increase in GTB is seen in the presence of Mn^{2+}.

We would like to put forward the hypothesis that Mg^{2+} instead of Mn^{2+} functions as the natural cofactor of GTB. Our hypothesis is based on the observation that, at physiological GTB concentrations as estimated above, the rate of catalysis of GTB is practically identical for Mn^{2+}, Mg^{2+}, and Ca^{2+} (Fig. 7*B*). Our experiments, in conjunction with the estimated GTB concentration in the cell, suggest that Michaelis-Menten conditions, *i.e.* rather low protein concentrations, do not reflect *in vivo* conditions well (40, 41), and therefore, activation of GTB by Mg^{2+} could be as effective as activation by Mn^{2+}. Intracellular metal ion concentrations are essential to establish which cation serves as the "natural" cofactor. Although the cellular concentrations of Ca^{2+}, Mg^{2+}, and Mn^{2+} are 1–2 mM, 20 mM, and ~12 μM, respectively (45), only 0.1 μM Ca^{2+}, 500 μM Mg^{2+}, and <1 μM Mn^{2+} may be considered to circulate free in solution. Therefore, it appears that the *in vivo* role of Mn^{2+} as an essential cation for many glycosyltransferases is questionable unless the metal ion is very tightly bound to the enzyme. Our experiments suggest that the activity of GTB is promoted by Mg^{2+} rather than by Mn^{2+} because the concentration of free Mg^{2+} ions is ~500 times higher than that of Mn^{2+}, whereas both metal ions increase the activity of GTB by the same order of magnitude at protein concentrations above ~3 μM. In the Golgi, free Ca^{2+} concentrations reach concentrations of 10 μM (46). Therefore, the concentration of Ca^{2+} is >10-fold lower than that of Mg^{2+}, and the influence of Ca^{2+} should be negligible under physiological conditions. However, although our results indicate that, under the conditions found in the *trans*-Golgi, Mn^{2+} is not an essential cation for the enzymatic activity of GTB, it may well be that local protein and metal ion concentrations in the cell differ from our rough approximations.

Finally, it is useful to compare these findings with results obtained on a bifunctional enzyme, UDP-GlcNAc 2-epimerase/ManNAc kinase (13, 14). For sugar kinases, it has been suggested that Mg^{2+} shields the negative charges of the β- and γ-phosphate groups of ATP and thus facilitates the nucleophilic attack of the sugar hydroxyl group on the γ-phosphate (17, 47). Because the reaction catalyzed by GTB occurs without nucleophilic attack on the phosphate groups, it is not very likely that the metal ions are "directly" involved in the enzyme reaction. This difference is illustrated by the observation that a small amount of Mg^{2+} results in a 15-fold increase in ManNAc kinase activity (14), whereas the same amount of Mg^{2+} results in only a 3-fold increase in GTB activity. On the other hand, the UDP-GlcNAc 2-epimerase reaction, a "retaining transferase-like reaction," is not influenced by the presence of metal ions. This is in accordance with our findings for GTB and lends further credit to the hypothesis that Mg^{2+} plays an important role in regulating GTB activity *in vivo*.

To summarize, our work reveals a number of novel aspects concerning mechanistic features of GTB catalysis at the atomic level. Using a fragment-based approach, it was possible to identify the contribution of the individual parts of the donor substrate for specific recognition by the enzyme, as illustrated in Fig. 8. These data significantly extend prior x-ray (9) and associated NMR[5] studies and, at the same time, encourage new experimental approaches that will target possible conformational changes in the enzyme associated with the binding of donor substrates.

REFERENCES

1. Gibson, R. P., Tarling, C. A., Roberts, S., Withers, S. G., and Davies, G. J. (2004) *J. Biol. Chem.* **279,** 1950–1955
2. Coutinho, P. M., Deleury, E., Davies, G. J., and Henrissat, B. (2003) *J. Mol. Biol.* **328,** 307–317
3. Paulson, J. C., and Colley, K. J. (1989) *J. Biol. Chem.* **264,** 17615–17618
4. Yamamoto, F.-I., Clausen, H., White, T., Marken, J., and Hakomori, S. (1990) *Nature* **345,** 229–233
5. Yamamoto, F.-I., and Hakomori, S. (1990) *J. Biol. Chem.* **265,** 19257–19262
6. Watkins, W. M. (1980) *Adv. Hum. Genetics* **10,** 1–136
7. Feizi, T. (1985) *Nature* **314,** 53–57
8. Singhal, A., and Hakomori, S. (1990) *BioEssays* **12,** 223–230
9. Patenaude, S. I., Seto, N. O. L., Borisova, S. N., Szpacenko, A., Marcus, S. L., Palcic, M. M., and Evans, S. V. (2002) *Nat. Struct. Biol.* **9,** 685–690
10. Mayer, M., and Meyer, B. (1999) *Angew. Chem. Int. Ed. Engl.* **38,** 1784–1788
11. Mayer, M., and Meyer, B. (2001) *J. Am. Chem. Soc.* **123,** 6108–6117
12. Peters, T., and Meyer, B. (2003) *Angew. Chem. Int. Ed. Engl.* **42,** 864–890
13. Blume, A., Benie, A. J., Stolz, F., Schmidt, R. R., Reutter, W., Hinderlich, S., and Peters, T. (2004) *J. Biol. Chem.* **279,** 55715–55721
14. Benie, A. J., Blume, A., Schmidt, R. R., Reutter, W., Hinderlich, S., and Peters, T. (2004) *J. Biol. Chem.* **279,** 55722–55727
15. Seto, N. O. L., Palcic, M. M., Hindsgaul, O., Bundle, D. R., and Narang, S. A. (1995) *Eur. J. Biochem.* **234,** 323–328
16. Kamath, V. P., Seto, N. O. L., Compston, C. A., Hindsgaul, O., and Palcic, M. M. (1999) *Glycoconj. J.* **16,** 599–606
17. Pollard-Knight, D., Potter, B. V., Cullis, P. M., Lowe, G., and Cornish-Bowden, A. (1982) *Biochem. J.* **201,** 421–423
18. Benie, A. J., Moser, R., Bauml, E., Blaas, D., and Peters, T. (2003) *J. Am. Chem. Soc.* **125,** 14–15
19. Cantor, C. R., and Schimmel, P. R. (1980) *Biophysical Chemistry Part III: The Behavior of Biological Macromolecules*, W. H. Freeman & Co., New York
20. Seto, N. O. L., Compston, C. A., Evans, S. V., Bundle, D. R., Narang, S. A., and Palcic, M. M. (1999) *Eur. J. Biochem.* **259,** 770–775
21. Schwyzer, M., and Hill, R. L. (1976) *J. Biol. Chem.* **252,** 2346–2355

22. Biet, T., and Peters, T. (2001) *Angew. Chem. Int. Ed. Engl.* **40,** 4189–4192
23. Ramakrishnan, B., Balaji, P. V., and Qasba, P. K. (2002) *J. Mol. Biol.* **318,** 491–502
24. Boix, E., Swaminathan, G. J., Zhang, Y., Natesh, R., Brew, K., and Acharya, K. R. (2001) *J. Biol. Chem.* **276,** 48608–48614
25. Gastinel, L. N., Bignon, C., Misra, A. K., Hindsgaul, O., Shaper, J. H., and Joziasse, D. H. (2001) *EMBO J.* **20,** 638–649
26. Boix, E., Zhang, Y., Swaminathan, G. J., Brew, K., and Acharya, K. R. (2002) *J. Biol. Chem.* **277,** 28310–28318
27. Heissigerová, H., Breton, C., Moravcová, J., and Imberty, A. (2003) *Glycobiology* **13,** 377–386
28. Seto, N. O. L., Compston, C. A., Szpacenko, A., and Palcic, M. M. (2000) *Carbohydr. Res.* **324,** 161–169
29. Marcus, S. L., Polakowski, R., Seto, N. O. L., Leinala, E., Borisova, S., Blancher, A., Roubinet, F., Evans, S. V., and Palcic, M. M. (2003) *J. Biol. Chem.* **278,** 12403–12405
30. Keppler, D. O., Rudigier, J. F., Bischoff, E., and Decker, K. F. (1970) *Eur. J. Biochem.* **17,** 246–253
31. Bernisone, P. M., and Hirschberg, C. B. (2000) *Curr. Opin. Struct. Biol.* **10,** 542–547
32. Norambuena, L., Marchant, L., Bernisone, P., Hirschberg, C. B., Silva, H., and Orellana, A. (2002) *J. Biol. Chem.* **277,** 32923–32929
33. Suda, T., Kamiyama, S., Suzuki, M., Kikuchi, N., Nakayama, K., Narimatsu, H., Jigami, Y., Aoki, T., and Nishihara, S. (2004) *J. Biol. Chem.* **279,** 26469–26474
34. Kuhn, N. J., and White, A. (1977) *Biochem. J.* **168,** 423–433
35. Blume, A., Chen, H., Reutter, W., Schmidt, R. R., and Hinderlich, S. (2002) *FEBS Lett.* **521,** 127–132
36. Powell, J. T., and Brew, K. (1976) *J. Biol. Chem.* **251,** 3645–3652
37. Boeggeman, E., and Qasba, P. K. (2002) *Glycobiology* **12,** 395–407
38. Ramakrishnan, B., Boeggeman, E., Ramasamy, V., and Qasba, P. K. (2004) *Curr. Opin. Struct. Biol.* **14,** 593–600
39. Zhang, Y., Wang, P. G., and Brew, K. (2001) *J. Biol. Chem.* **276,** 11567–11574
40. Schnell, S., and Maini, P. K. (2000) *Bull. Math. Biol.* **62,** 483–499
41. Grima, R., and Schnell, S. (2006) *Biophys. Chem.* **124,** 1–10
42. Kleinig, H., and Sitte, P. (1992) *Zellbiologie*, 3rd Ed., Gustav Fischer Verlag, Jena, Germany
43. Weibel, E. R., Stäubli, W., Gnägi, H. R., and Hess, F. A. (1969) *J. Cell Biol.* **42,** 68–91
44. Schwyzer, M., and Hill, R. L. (1977) *J. Biol. Chem.* **252,** 2338–2345
45. Brinkworth, R. I., Hanson, R. W., Fullin, F. A., and Schramm, V. L. (1981) *J. Biol. Chem.* **256,** 10795–10802
46. Strayle, J., Pozzan, T., and Rudolph, H. K. (1999) *EMBO J.* **17,** 4733–4743
47. Lowe, G., and Potter, B. V. (1981) *Biochem. J.* **199,** 227–233

Fragment-based Screening of the Donor Substrate Specificity of Human Blood Group B Galactosyltransferase Using Saturation Transfer Difference NMR

Astrid Blume, Jesus Angulo, Thorsten Biet, Hannelore Peters, Andrew J. Benie, Monica Palcic and Thomas Peters

J. Biol. Chem. 2006, 281:32728-32740.
doi: 10.1074/jbc.M600424200 originally published online August 21, 2006
